OPEN ACCESS

Kashf Journal of Multidisciplinary Research
Vol: 02 - Issue 1 (2025)
P-ISSN: 3007-1992 E-ISSN: 3007-200X
https://kjmr.com.pk

ENHANCING SOLAR CELL EFFICIENCY: A COMPREHENSIVE STUDY ON THE OPTO-ELECTRICAL PROPERTIES OF CUINALSE2 THIN FILMS AS AN ABSORBER LAYER

Muhammad Waqas
Centre of Excellence in Solid State Physics, University of the Punjab,Pakistan
Muhammad Sajid
Institute of Microscale Optoelectronics, Optical Engineering, Shenzhen University, Shenzhen, 518055, Guangdong Province, China
Maneeb Ur Rehman
Department of Physics, Faculty of Basic and Applied Sciences (FBAS), International Islamic University (IIU), H-10, Islamabad, 44000, Pakistan
Ayesha Amin
Department of Chemistry, Government College University Faisalabad, Pakistan
Muhammad Rehan
Department of Physics, The University of Lahore, Sub-campus Sargodha, 40100, Pakistan
Amna Abrar
Department of Chemistry, School of Science, Tianjin Key Laboratory of Molecular Optoelectronic Science, Tianjin University, Tianjin 300072, China
Basit Ahmad
Department of Electrical Engineering, NFC (Institute of Engineering and Technology) Multan,Pakistan
Anoosha Sajjad
Chemistry Department, Islamia College University, Peshawar 25000, Pakistan
Muhammad Shahab
Department of Physics, Ghazi University, Dera Ghazi Khan, Pakistan
Shahid Ashraf
Department of Physics, University of Agriculture Faisalabad, 38000, Faisalabad, Pakistan

Corresponding author: Muhammad Waqas (m.waqas.pu@gmail.com)

Article Info

Abstract

CIAS (CuInAlSe2) thin films were prepared by 1-step electrodeposition on ITO coated glass substrate by varying deposition potential to obtain low cost, uniform and compact crystallinity at room temperature. The 200ml solution has been prepared and operated at 0.55V to 0.95V deposition potentials. CIAS solution has been prepared at different molarity ratios varying from 0.1M to 1.0M solution and optimum results obtained at 0.5M molar solution. The results obtained from cyclic voltammetry reveals that quaternary compound having different reduction potential can be deposited in potential range 0.5V to 0.95V. XRD technique were used to study the structural, morphological properties of thin films that shows the strong evident of its crystalline nature having tetragonal pure phase with preferred orientation at (400) plane. The result showed that single phase having good stoichiometry can be produced in this potential range. The optical properties studied by ellipsometry technique revealed that the films are highly absorbing in visible and visible-infrared region by increasing deposition potential. The band gap calculation form absorption spectra were maintained at 1.11 to 1.32 eV which was excellent for good absorbing solar materials. Hall effect application van der pauw method used for electrical properties which show promising results for production of electricity by solar cells. The variation of deposition potential offers very effective change in band gap. Structural, morphological, electrical and optical properties were carried out to establish the suitability of thin films for solar cells fabrication.

Keywords: *CIAS (CuInAlSe2), Thin film, Solar cells, Ellipsometry, Electrodeposition.*

Introduction

The chalcopyrite CIAS ($CuInAlSe_2$) as an absorbing layer for cells emerged out as viable contender for low cost and highly efficient thin films. For the enhancement of efficiency a previous work reported at laboratory level with efficiency 19.9% with Cu (In, Ga)Se_2 [1]. CIAS is regarding as prominent contender for replacing Gallium and Sulphur because it required lower alloy content to match their band gaps. Also, Al is easily available and cost-friendly which will reduce the cost of the solar cells to prominent extent. This indicate that when $CuInSe_2$ is alloyed with Al than Ga then fluctuation of lattice parameters are comparatively smaller [2].

A lot of work reported on CIAS in last 2 decades using vacuum based processes like sputtering, co-evaporation, salinization [3-5]. The several research organizations reported that maximum efficiency obtained by CIAS was 16.9% [4, 5]. They are created by vacuum methods, but they are difficult to scale because of high manufacturing costs and poor material use efficiency. As a result of these benefits, the electro-deposition procedure must be beneficial for creating CIAS films: Low temperature production, low cost, large area, non-vacuum manufacturing and little material waste [6].

However, the electro-deposition of quaternary alloy is slightly challenging due to a large variation in the deposition potential of the solution components and the likelihood of the formation of intermediary phases during electro-deposition. The one-step electro-deposition approach is the most probable electrochemical method for synthesizing CIS-based films for applications involving solar cells such as CIS, CIGS, and CIAS. The variation in electrolyte concentrations is constrained by the associated plating potential of each element. The reduction potentials of each element in solutions are ascertained via cyclic voltammetry analysis.

In this research work, we investigated the variation of deposition potential to study the properties of CIAS thin film material grown at fixed molarity 0.5M and having the acidic pH =2 by the process of one-step electro-deposition with two electrode system without adding the any complexing agent.

2-Experimental details:

Indium tin oxide was coated on glass substrate to make it conducting for thin film deposition by electro-deposition method. First of all, substrate was cleaned by dipping it in acetone and then IPA (Isopropyl alcohol) and then putt into the ultrasonic bath for 20 minutes each time. The electrolyte solution comprising Cucl2, $InCl_3$, $AlCl_3$, and SeO_2 dissolved in de-ionized water and 200 ml solution is prepared. Samples are prepared at molarity ranges 0.1 to 1.0M but the most preferred sample obtained at 0.5M which was further used results evaluation. Single-step electro-deposition technique by using two electrodes without complexing agent was used to prepare thin films by varying deposition potential 0.55V, 0.65V, 0.75V, 0.85V and 0.95V.

Block Diagram:

Figure 1.1 Diagram of experimental steps

The reduction of copper, indium, aluminum and selenium occurs by the following reaction mechanism [7].

For Copper: $Cu^{+2} + 2e \rightarrow Cu_s$

For Indium: $In^{+3} + 3e \rightarrow In_s$

For Aluminium: $Al^{+3} + 3e \rightarrow Al_s$

For Selinide: $HSeO_2^{+} + 4H^{+} + 4e + OH^{-1} \rightarrow H_2SeO_3 + 4H^{+} + 4e \rightarrow Se_s + 3H_2O$

The value at which all elements are co-deposited is at reduction potential 0.05ml.

By scanning the potential between two or more acting values, cyclic voltammetry was utilized to quantify the current of a redox active analyte. Structural properties were analyzed by X-rays diffractometer model Bruker D-8 advance with Cu-kα characteristics x-rays having wavelength 1.5406 **Å.** Crystallite size was calculated by Scherer's formula.

$$D = 0.9\frac{\lambda}{\beta \cos\theta} ,$$

Where 'D' is Crystallite size,0.9 is shape constant for tetragonal, 'λ' is the wavelength of X-rays, 'β' is the full width at half maximum (FWHM) and 'θ' is the Bragg's angle. Optical properties were analyzed by Spectroscopic Ellipsometry model no. **J. Whoolam M-2000**. Hall Effect application Van der Pauw method was used to study the electrical properties of the thin film material.

Results and Discussion:

3.1 Cyclic Voltammetry measurements

The CV curve of a quaternary electrolyte (Figure 1) shows the main reduction potential of Cu and Se are at 0.34V and -0.115V respectively. The possible results indicating from Figure 1 considering the literature [7] that the reduction potential of In and Al (active metals) are 0.34 and -0.662V, respectively. Higher rate of reduction of Cu, In and Al can be shown with comparison of Se. The lower conductivity of Selenium decreases the current density and deposition rate. Interestingly, the CV measurement cycle for quaternary electrolyte shows the change in reduction potential by increasing CV cycle [7, 8].

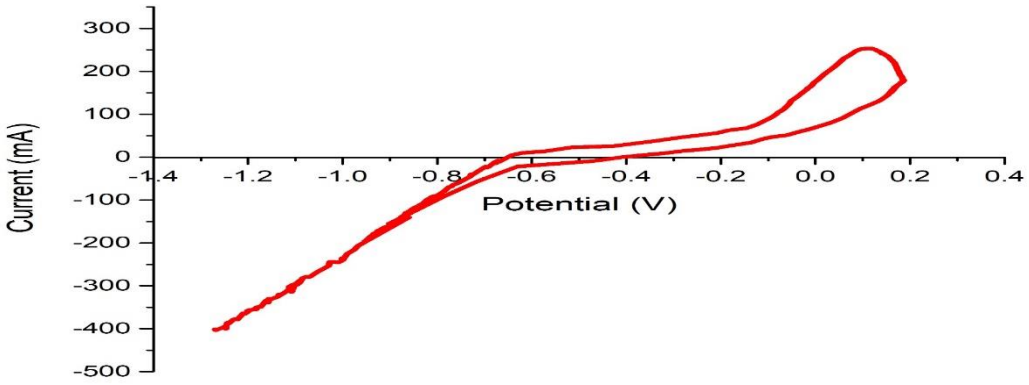

Figure 1 Recorded CV curve for Quaternary electrolyte (Cu, In, Al and Se_2)

With the help of CV measurements, it illustrated that quaternary thin film can be deposited at the deposition range 0.5V to 1.0V. The potential chemical reactions and formation potential of quaternary CIAS films were examined using cyclic voltammetry measurements.

3.2 X-Ray Diffraction:

To study the structural properties of prepared material X-ray diffraction was carried out with Bruker D-8 Modern. The XRD peaks (Figure 3.2) shows the polycrystalline quaternary crystal having preferred orientations along (400), (331), (620), (551) and (642) matched with JCPDS card no. 00-026-0499 CIAS material.

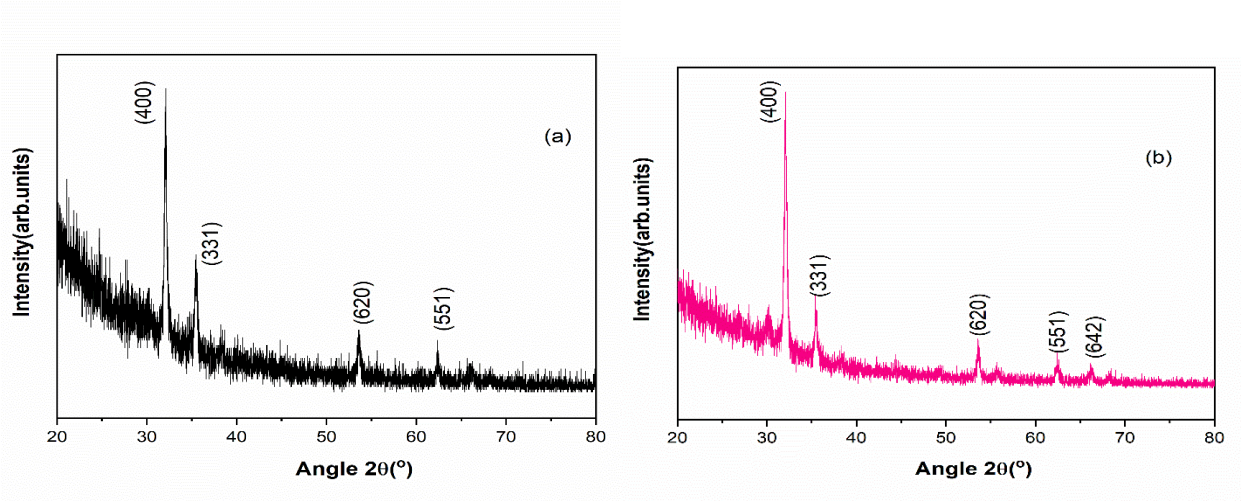

Figure 2.1 XRD patterns a) 0.55V and b) 0.65V deposition potential

We can observe that no supplementary peaks due to impurity or secondary phase appears. (400) planes have large intensity which is due to large number of similar planes interfere constructively with same d-spacing at this specific angle, also we observed that 2nd pattern have sharper peak of (400) than first one which shows that it has large crystallinity and low FWHM value. We observed from these two patterns that crystallite size of thin film increases due to increase in deposition potential.

Following formulas are used to calculate the 'β'which represents FWHM, 'D' crystallite size, 'δ' dislocation density and 'ε' strain produced in a material.

$\boldsymbol{\beta} = 2\theta_2 - 2\theta_1$

$$\mathbf{D} = \frac{k\lambda}{\beta \cos\theta}$$

$$\boldsymbol{\delta} = \frac{1}{D^2}$$

$$\boldsymbol{\varepsilon} = \frac{\beta}{4\tan\theta}$$

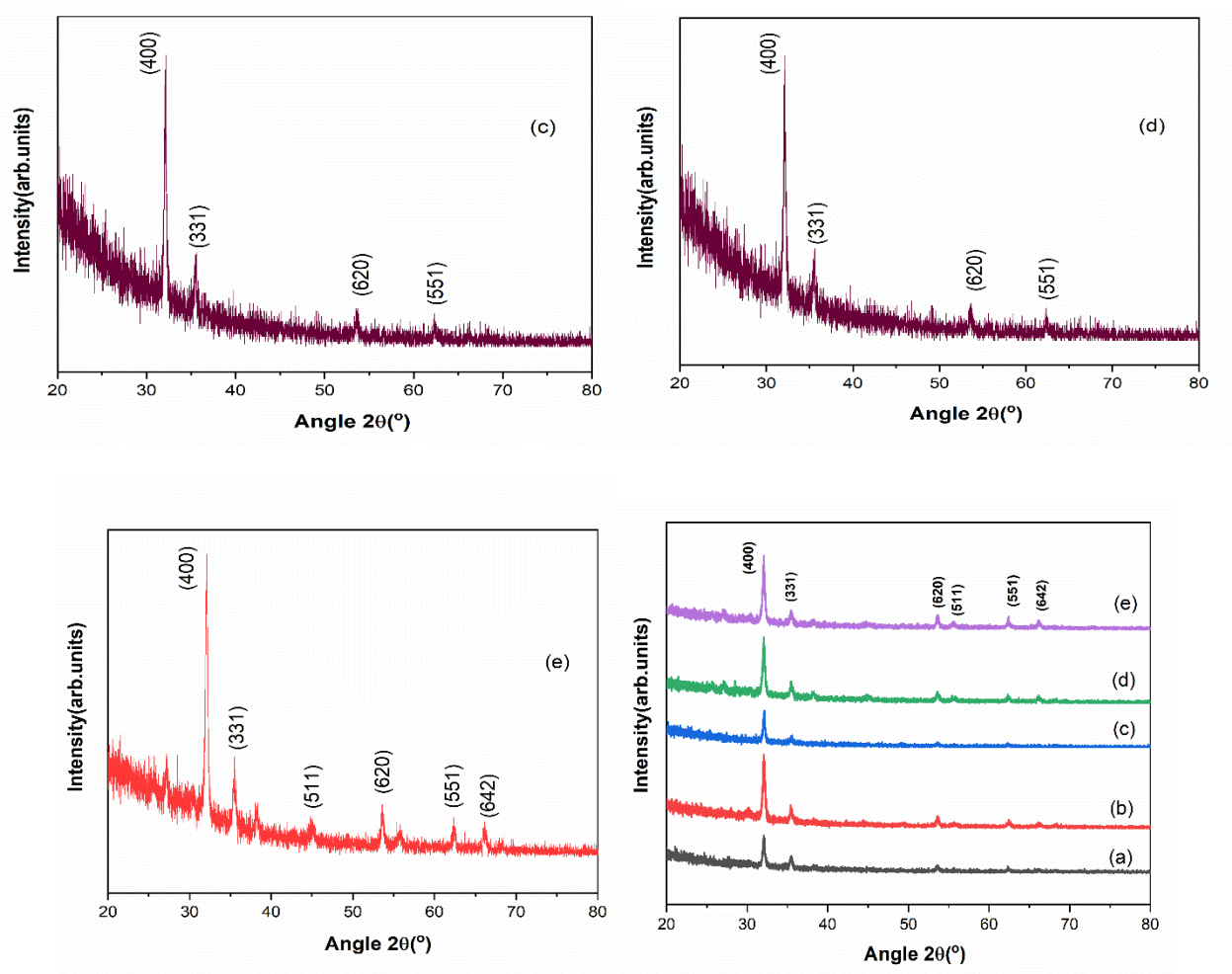

Figure 2.2 shows the XRD patterns at c) 0.75V, d) 0.85V, e) 0.95V and the compiled XRD graph.

We had seen that crystallinity increased as deposition potential climbed in the previous two patterns, but here we see a distinct paradigm at 0.75V deposition potential where FWHM rises, resulting in a decline in crystallite size due to material re-structuring at this deposition potential. Figure 3.2(d) depicts an extremely intense and abrupt peak suggesting a large number of crystallite sizes, indicating that the material is nearing stability. My best sample is also 0.85V, showing a very solid structure. Also we have observed a slight shift towards left side at higher deposition potential which is due to production of strain at higher value [9].

3.3 Optical analysis:

Optical properties of CIAS thin films were investigated with the help of Ellipsometry spectroscopic model **J.Whoolam M-2000** [16]**.** Transmittance, Absorbance by thin films and band gap our major concern. The quaternary Cu (In, Al) Se2 semiconductor possesses a direct band gap, the energy band gap Eg may be estimated by taking the x-intercept of the linear extrapolation of the curve displaying the change' α' versus photon energy using the relationship [10].

$$\boldsymbol{\alpha}(h\nu) = \frac{c}{h\nu}(h\nu - E_g)^{1/2}$$

where '**α' is** absorption co-efficient, 'hν' is the incident photon energy, 'E_g ' is the band gap and 'c' is the constant depends on transition nature, effective mass and refractive index.

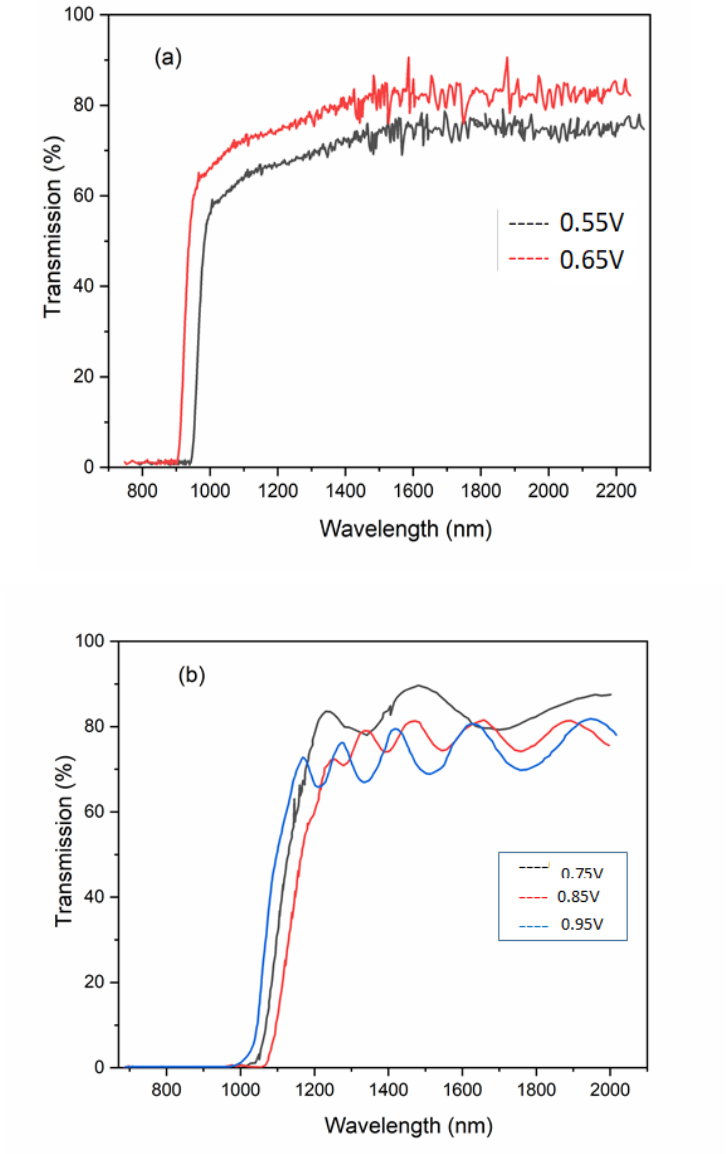

Figure 3 Transmission graph by varying deposition potential, a) 0.55V, 0.65V b) 0.75V, 0.85V and 0.95V.

The transmission graph shows that the maximum transmission occurs at 0.65V and can reach 85%. This is owing to the significantly larger band gap (1.32) in compared to the 0.55V band gap (1.30)[11]. We may conclude that as the band gap widens, so does transmission[12]. The peaks and dips in the graph are created by constructive and destructive interference that happens prior to light entering the sensor[13]. It can also occur as a result of a detector fault. The fundamental absorption edge for 0.55V is smaller than the other, indicating considerable absorption at 0.65V deposition potential. At 0.75V potential, a disorder variation develops owing to a quick reduction in band gap (from 1.32 to 1.12), generating enhanced transmission since the material's structure is not stable at this potential. At my ideal sample, a considerable absorption range is plainly seen, showing great agreement for the absorber layer. After that a small variation occurs which is due to increase in band gap which causes decrease in absorption [14].

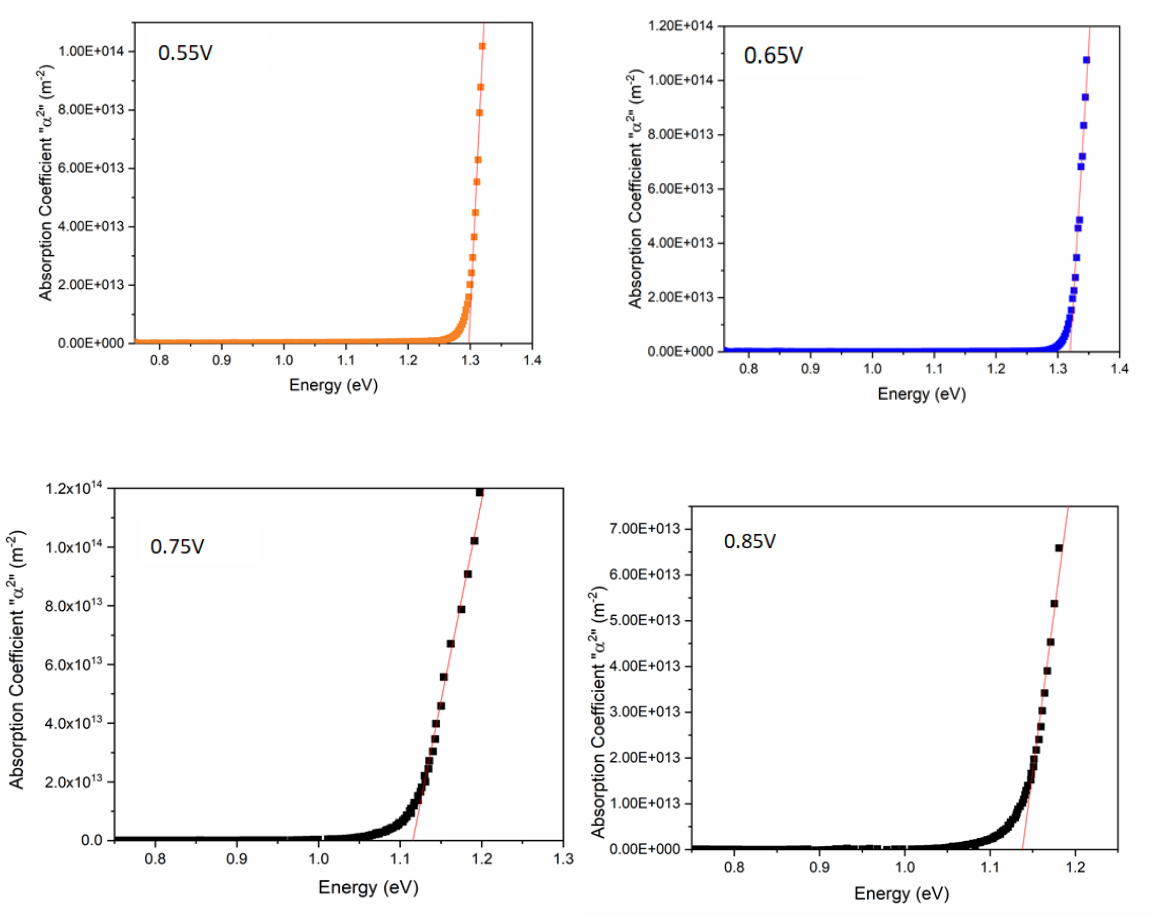

Figure 4 Band gap graph at 0.55V, 0.65v, 0.75V and 0.85V

Extrapolating the graph's linear part yields the band gap. The graph below depicts the connection between the absorption co-efficient and photon energy [15]. The material's band gap is 1.3 at 0.55V, and when the deposition potential increases, so does the band gap, which is connected to the increase in crystallite size stated in XRD. Crystallinity increases the number of grains in a lattice, which minimizes the grain boundary[16]. The band gap will widen as a result of this reduction. The graph of 'α^2' and energy demonstrates that we obtained a direct band gap material for optimal absorption. Due to lattice re-structuring or re-arrangements, the band gap drops dramatically at 0.75V potential. Furthermore, when deposition potential increases, so does the band gap, which is linked to the previously mentioned increase in crystallite size.

The absorption co-efficient can be found with well-known equation.

$$\alpha=\frac{1}{t}\ln\left[\frac{2TR^2}{-(1-R)^2+\sqrt{4R^2T^2+(1-R)^4}}\right]$$

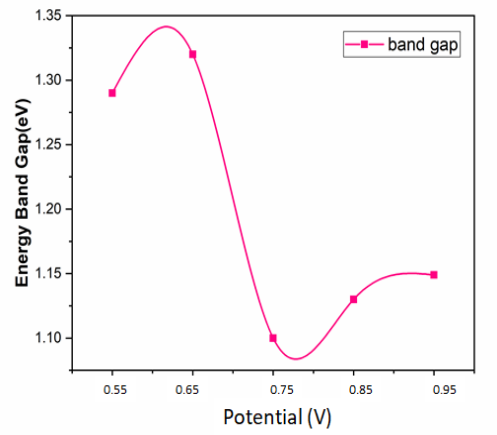

Figure 4.2 Graph between energy band gap and potential v

The entire variation in the band gap as a function of deposition potential is shown in Figure 3.3. The band gap rises with potential; however, there is a significant dip at 0.75V, which is due to the small crystallite size at this molarity, as indicated in XRD[16]. Increase the band gap by increasing the deposition potential; however, this range is already stated for a suitable absorber layer.

3.4 Electrical Properties:

The electrical properties was analyzed with the help of Hall effect application; Van Der Pauw method[17]. Room-temperature Hall measurements using the four-point probe technique, the conduction type, carrier density, carrier mobility, and electrical resistivity of the generated Cu(In, Al)Se2 films are measured [7].

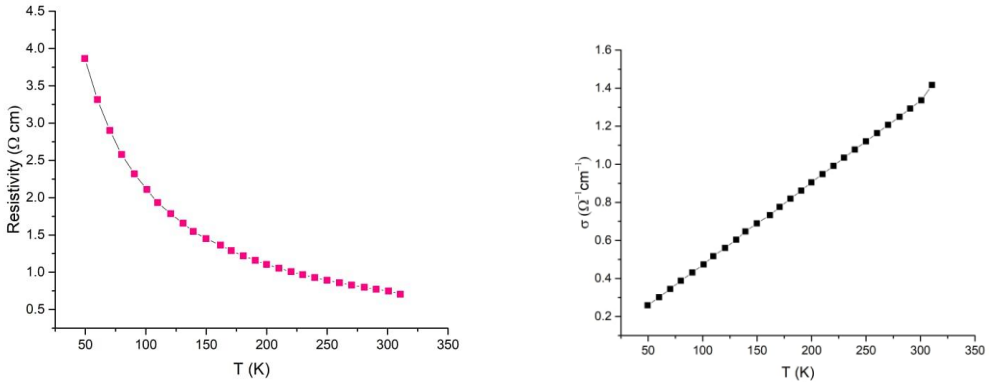

Figure 5.1 graph between resistivity and conductivity with temperature variation

We can explain decrease in resistivity by increasing temperature by Petritz's barrier model. According to this idea, crystallites do not grow large enough at low temperatures, but grow large enough at high temperatures to minimize the inter-crystalline barrier[18]. As a result, the inter-crystalline barriers are comparatively thin, reducing resistivity. The p-type hot probe technique is used in all films, and it is apparent that conductivity increases with temperature[19].

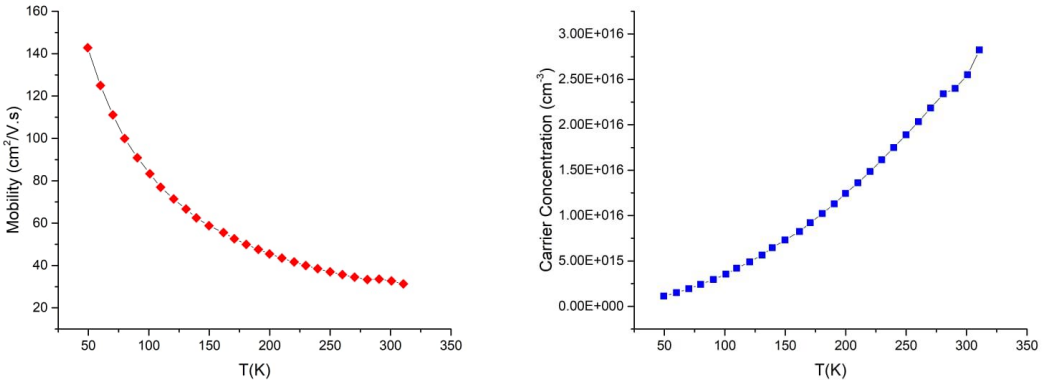

Figure 5.2 graph between mobility and carrier concentration with temperature

The graph shows that as temperature rises, so does carrier concentration. Because CIAS is a negative temperature semiconductor, more carriers enter the conduction band as temperature rises, increasing carrier concentration. As shown in the graph, carrier mobility diminishes as carrier concentration increases [20, 21].

CONCLUSION

CIAS thin films were deposited at different deposition potential by the process of electro-deposition at room temperature to. The results obtained from cyclic voltammetry reveals that quaternary compound having different reduction potential can be deposited in potential range 0.5V to 0. 95V.These thin film's structure were analyzed by XRD technique which showed that highest intensity peaks identified at (400) plane, evident of tetragonal pure phase and low-cost thin films. The maximum crystallite size was observed at 0.85V deposition potential which revealed that at this potential highly brittle thin films material can be obtained. The optical properties were analyzed by ellipsometry spectrometer which revealed that synthesized thin films have band gap range from 1.11 to 1.31 eV at different deposition potential. This range of band gap was excellent for optical absorbance materials. The transmission graph showed that fundamental absorption edge was formed at 850 nm. The tunable band gap observed in this prepared thin film. Hall Effect measurements show that resistivity decrease with increase in temperature which causes an increase in conductivity of thin film. The p-type hot probe technique is used in all films, and it is apparent that conductivity increases with temperature.

References:

1. Shafarman, W.N., R. Klenk, and B.E. McCandless, *Device and material characterization of Cu (InGa) Se2 solar cells with increasing band gap.* Journal of Applied Physics, 1996. **79**(9): p. 7324-7328.
2. Sugiyama, M., et al., *Growth of single-phase Cu (In, Al) Se2 photoabsorbing films by selenization using diethylselenide.* Thin Solid Films, 2009. **517**(7): p. 2175-2177.
3. Yamada, S., et al., *Effect of Al addition on the characteristics of Cu (In, Al) Se2 solar cells.* Journal of crystal growth, 2009. **311**(3): p. 731-734.
4. Hayashi, T., et al., *Effect of composition gradient in Cu (In, Al) Se2 solar cells.* Solar Energy Materials and Solar Cells, 2009. **93**(6-7): p. 922-925.
5. Yun, J.H., et al., *Formation of CuIn1-xAlxSe2 Thin Films by Selenization of Metallic Precursors in Se Vapor.* Solid State Phenomena, 2007. **124**: p. 975-978.
6. Marsillac, S., et al., *High-efficiency solar cells based on Cu (InAl) Se 2 thin films.* Applied Physics Letters, 2002. **81**(7): p. 1350-1352.
7. Meglali, O., et al., *The effect of Al and In concentrations on the properties of electrodeposited Cu (In, Al) Se2 using two electrode system without the addition of complexing agents.* Optik, 2017. **140**: p. 709-717.
8. Ganjkhanlou, Y., et al., *Electrodeposition of CuIn (Al) Se 2-based thin films on various substrates.* Journal of Materials Science: Materials in Electronics, 2020. **31**: p. 10241-10250.
9. Ganjkhanlou, Y., et al., *Effect of pH on the electrodeposition of Cu (In, Al) Se 2 from aqueous solution in presence of citric acid as complexing agent.* Surface Review and Letters, 2015. **22**(05): p. 1550057.
10. López-García, J., C. Maffiotte, and C. Guillén, *Wide-bandgap CuIn1− xAlxSe2 thin films deposited on transparent conducting oxides.* Solar Energy Materials and Solar Cells, 2010. **94**(7): p. 1263-1269.
11. Meng, X., et al., *Structural, optical and electrical properties of Cu2FeSnSe4 and Cu (In, Al) Se2 thin films.* Materials Science in Semiconductor Processing, 2015. **39**: p. 243-250.
12. Cao, H., et al., *Investigation of microstructural and optical properties of Cu (In, Al) Se2 thin films with various copper content.* Journal of Alloys and Compounds, 2015. **651**: p. 208-213.
13. Riaz, S., S. Batool, and S. Naseem, *Structural and Optical properties of CIAGS thin films.* Advances in Nano, Biomechanics, Robotics, and Energy Research, 2013.
14. Huang, K.-C., et al., *Effect of [Al] and [In] molar ratio in solutions on the growth and microstructure of electrodeposition Cu (In, Al) Se2 films.* Applied surface science, 2013. **273**: p. 723-729.
15. Parihar, U., et al., *Effect of film thickness and annealing on the structural and optical properties of CuInAlSe2 thin films*. 2013, Sumy State University.
16. Mor, S., et al., *Ultrafast electronic band gap control in an excitonic insulator.* Physical review letters, 2017. **119**(8): p. 086401.
17. Náhlík, J., I. Kašpárková, and P. Fitl, *Study of quantitative influence of sample defects on measurements of resistivity of thin films using van der Pauw method.* Measurement, 2011. **44**(10): p. 1968-1979.
18. Kavitha, B. and M. Dhanam, *Transport properties of copper indium aluminum selenide thin films deposited by successive Ionic layer adsorption and reaction.* Materials science in semiconductor processing, 2013. **16**(2): p. 495-503.
19. Amal, M., et al., *Critical Condition in CuInAlSe 2 Solar Cell Absorbers.* Telkomnika, 2016. **14**(3).
20. Zhou, L.M., S.M. Wu, and J.P. Yu, *Influence of Al Concentration on Performance of Cu (In, Al) Se2 (CIAS) Films.* Advanced Materials Research, 2012. **557**: p. 1879-1883.

21. Sujarwata, S., et al., *Critical condition in CuInAlSe2 growth of solar cell absorber*. TELKOMNIKA (Telecommunication Computing Electronics and Control), 2016. **14**(3): p. 867-872.